Inhibitory effect of eslicarbazepine acetate and S-licarbazepine on $Na_v1.5$ channels

Theresa K. Leslie[1], Lotte Brückner [1], Sangeeta Chawla[1,2], William J. Brackenbury[1,2*]

[1]Department of Biology, University of York, Heslington, York, YO10 5DD, UK

[2]York Biomedical Research Institute, University of York, Heslington, York, YO10 5DD, UK

*** Correspondence:** Dr William J. Brackenbury, Department of Biology and York Biomedical Research Institute, University of York, Wentworth Way, Heslington, York YO10 5DD, UK. Email: william.brackenbury@york.ac.uk. Tel: +44 1904 328284.

Keywords: Anticonvulsant, cancer, epilepsy, eslicarbazepine acetate, $Na_v1.5$, S-licarbazepine, voltage-gated Na^+ channel.

Abstract

Eslicarbazepine acetate (ESL) is a dibenzazepine anticonvulsant approved as adjunctive treatment for partial-onset epileptic seizures. Following first pass hydrolysis of ESL, S-licarbazepine (S-Lic) represents around 95 % of circulating active metabolites. S-Lic is the main enantiomer responsible for anticonvulsant activity and this is proposed to be through the blockade of voltage-gated Na^+ channels (VGSCs). ESL and S-Lic both have a voltage-dependent inhibitory effect on the Na^+ current in N1E-115 neuroblastoma cells expressing neuronal VGSC subtypes including $Na_v1.1$, $Na_v1.2$, $Na_v1.3$, $Na_v1.6$ and $Na_v1.7$. ESL has not been associated with cardiotoxicity in healthy volunteers, although a prolongation of the electrocardiographic PR interval has been observed, suggesting that ESL may also inhibit cardiac $Na_v1.5$ isoform. However, this has not previously been studied. Here, we investigated the electrophysiological effects of ESL and S-Lic on $Na_v1.5$ using whole-cell patch clamp recording. We interrogated two model systems: (1) MDA-MB-231 metastatic breast carcinoma cells, which endogenously express the 'neonatal' $Na_v1.5$ splice variant, and (2) HEK-293 cells stably over-expressing the 'adult' $Na_v1.5$ splice variant. We show that both ESL and S-Lic inhibit transient and persistent Na^+ current, hyperpolarise the voltage-dependence of slow inactivation, and slow the recovery from channel inactivation. These findings highlight, for the first time, the potent inhibitory effects of ESL and S-Lic on the $Na_v1.5$ isoform, suggesting a possible explanation for the prolonged PR interval observed in patients on ESL treatment. Given that numerous cancer cells have also been shown to express $Na_v1.5$, and that VGSCs potentiate invasion and metastasis, this study also paves the way for future investigations into ESL and S-Lic as potential invasion inhibitors.

1 Introduction

Eslicarbazepine acetate (ESL) is a member of the dibenzazepine anticonvulsant family of compounds which also includes oxcarbazepine and carbamazepine (1). ESL has been approved by the European Medicines Agency and the United States Federal Drug Administration as an adjunctive treatment for partial-onset epileptic seizures (2). ESL is administered orally and rapidly undergoes first pass hydrolysis to two stereoisomeric metabolites, R-licarbazepine and S-licarbazeine (S-Lic; also known as eslicarbazepine; Figure 1A, B) (3-5). S-Lic represents around 95 % of circulating active metabolites following first pass hydrolysis of ESL and is the enantiomer responsible for

anticonvulsant activity (6, 7). S-Lic also has improved blood brain barrier penetration compared to R-licarbazepine (8). Although S-Lic has been shown to inhibit T type Ca^{2+} channels, its main activity is likely through blockade of voltage-gated Na^+ channels (VGSCs) (9, 10). ESL offers several clinical advantages over other older VGSC-inhibiting antiepileptic drugs, e.g. carbamazepine, phenytoin; it has a favourable safety profile (10, 11), reduced induction of hepatic cytochrome P450 enzymes (12), low potential for drug-drug interactions (13, 14), and takes less time to reach a steady state plasma concentration (15).

VGSCs are heteromeric ion channels composed of a pore-forming α subunit in association with one or more auxiliary β subunits, the latter modulating channel gating and kinetics in addition to functioning as cell adhesion molecules (16). There are nine α subunits ($Na_v1.1$-$Na_v1.9$), and four β subunits (β1-4) (17, 18). In postnatal and adult CNS neurons, the predominant α subunits are the tetrodotoxin-sensitive $Na_v1.1$, $Na_v1.2$ and $Na_v1.6$ isoforms (19) and it is therefore on these that the VGSC-inhibiting activity of ESL and S-Lic has been described. In the murine neuroblastoma N1E-115 cell line, which expresses $Na_v1.1$, $Na_v1.2$, $Na_v1.3$, $Na_v1.6$ and $Na_v1.7$, ESL and S-Lic both have a voltage-dependent inhibitory effect on the Na^+ current (10, 20). In this cell model, S-Lic has no effect on the voltage-dependence of fast inactivation, but significantly hyperpolarises the voltage-dependence of slow inactivation (10). S-Lic also has a lower affinity for VGSCs in the resting state than carbamazepine or oxcarbazepine, thus potentially improving its therapeutic window over first- and second-generation dibenzazepine compounds (10). In acutely isolated murine hippocampal CA1 neurons, which express $Na_v1.1$, $Na_v1.2$ and $Na_v1.6$ (21-23), S-Lic significantly reduces the persistent Na^+ current, a very slow-inactivating component ~1 % the size of the peak transient Na^+ current (24, 25). Moreover, in contrast to carbamazepine, this effect is maintained in the absence of β1 (24, 26).

In healthy volunteers, ESL has not been associated with cardiotoxicity and the QT interval remains unchanged on treatment (27). However, a prolongation of the PR interval has been observed (27), suggesting that caution should be exercised in patients with cardiac conduction abnormalities (13). Prolongation of the PR interval also suggests that ESL may also inhibit the cardiac $Na_v1.5$ isoform, although this has not previously been studied. $Na_v1.5$ is not only responsible for the initial depolarisation of the cardiac action potential (28), but is also expressed in breast and colon carcinoma cells, where the persistent Na^+ current promotes invasion and metastasis (29-32). Inhibition of $Na_v1.5$ with phenytoin or ranolazine decreases tumour growth, invasion and metastasis (33-35). Thus, it is of interest to specifically understand the effect of ESL on the $Na_v1.5$ isoform.

In the present study we investigated the electrophysiological effects of ESL and S-Lic on $Na_v1.5$ [1] endogenously expressed in the MDA-MB-231 metastatic breast carcinoma cell line, and [2] stably over-expressed in HEK-293 cells. We show that both ESL and S-Lic inhibit transient and persistent Na^+ current, hyperpolarise the voltage-dependence of slow inactivation, and slow the recovery from channel inactivation. These findings highlight, for the first time, the potent inhibitory effects of ESL and S-Lic on the $Na_v1.5$ isoform.

2 Materials and methods

2.1 Pharmacology

ESL (Tokyo Chemical Industry UK Ltd) was dissolved in DMSO to make a stock concentration of 67 mM. S-Lic (Tocris) was dissolved in DMSO to make a stock concentration of 300 mM. Both drugs were diluted to a working concentration of 300 μM in extracellular recording solution.

82 **2.2 Cell culture**

83 MDA-MB-231 cells and HEK-293 cells stably expressing $Na_v1.5$ (a gift from L. Isom, University of
84 Michigan) were grown in Dulbecco's modified eagle medium supplemented with 5 % FBS and 4
85 mM L-glutamine (36). Molecular identity of the MDA-MB-231 cells was confirmed by short tandem
86 repeat analysis (37). Cells were confirmed as mycoplasma-free using the DAPI method (38). Cells
87 were seeded onto glass coverslips 48 h before electrophysiological recording.

88 **2.3 Electrophysiology**

89 Plasma membrane Na^+ currents were recorded using the whole-cell patch clamp technique, using
90 methods described previously (32, 35, 39-41). Patch pipettes made of borosilicate glass were pulled
91 using a P-97 pipette puller (Sutter Instrument) and fire-polished to a resistance of 3-5 MΩ when
92 filled with intracellular recording solution. The extracellular recording solution for MDA-MB-231
93 cells contained (in mM): 144 NaCl, 5.4 KCl, 1 $MgCl_2$, 2.5 $CaCl_2$, 5.6 D-glucose and 5 HEPES
94 (adjusted to pH 7.2 with KOH). For the extracellular recording solution for HEK-293 cells
95 expressing $Na_v1.5$, the extracellular [Na^+] was reduced to account for the much larger Na^+ currents
96 and contained (in mM): 60 NaCl, 84 Choline Cl, 5.4 KCl, 1 $MgCl_2$, 2.5 $CaCl_2$, 5.6 D-glucose and 5
97 HEPES (adjusted to pH 7.2 with KOH). The intracellular recording solution contained (in mM): 5
98 NaCl, 145 CsCl, 2 $MgCl_2$, 1 $CaCl_2$, 10 HEPES, 11 EGTA, (adjusted to pH 7.4 with CsOH) (42).
99 Voltage clamp recordings were made at room temperature using a Multiclamp 700B amplifier
100 (Molecular Devices) compensating for series resistance by 40–60%. Currents were digitized using a
101 Digidata 1440A interface (Molecular Devices), low pass filtered at 10 kHz, sampled at 50 kHz and
102 analysed using pCLAMP 10.7 software (Molecular Devices). Leak current was subtracted using a
103 P/6 protocol (43). Extracellular recording solution ± drugs was applied to the recording bath at a rate
104 of ~1.5 ml/min using a ValveLink 4-channel gravity perfusion controller (AutoMate Scientific). Each
105 new solution was allowed to equilibrate in the bath for ~4 min following switching prior to recording
106 at steady state.

107 **2.4 Voltage clamp protocols**

108 Cells were clamped at a holding potential of -120 mV or -80 mV for ≥ 250 ms, dependent on
109 experiment (detailed in the Figure legends). Five main voltage clamp protocols were used, as
110 follows:

111 1. To assess the effect of drug perfusion and wash-out on peak current in real time, a simple one-
112 step protocol was used where cells were held at -120 mV or -80 mV for 250 ms and then
113 depolarised to -10 mV for 50 ms.

114 2. To assess the voltage-dependence of activation, cells were held at -120 mV for 250 ms and then
115 depolarised to test potentials in 10 mV steps between -120 mV and +30 mV for 50 ms.

116 3. To assess the voltage-dependence of steady-state inactivation, cells were held at -120 mV for 250
117 ms followed by prepulses for 250 ms in 10 mV steps between -120 mV and +30 mV and a test
118 pulse to -10 mV for 50 ms.

119 4. To assess use-dependent block, cells were held at -120 mV for 250 ms and then depolarised to 0
120 mV at a frequency of 50 Hz, with each depolarisation pulse lasting 50 ms.

5. To assess recovery from fast inactivation, cells were held at -120 mV for 250 ms, and then depolarised twice to 0 mV for 25 ms, returning to -120 mV for the following intervals between depolarisations (in ms): 1, 2, 3, 5, 7, 10, 15, 20, 30, 40, 50, 70, 100, 150, 200, 250, 350, 500.

2.5 Curve fitting and data analysis

To study the voltage-dependence of activation, current-voltage (I-V) relationships were converted to conductance using the following equation:

$G = I / (V_m - V_{rev})$, where G is conductance, I is current, V_m is the membrane voltage and V_{rev} is the reversal potential for Na^+ derived from the Nernst equation.

The voltage-dependence of conductance and availability were normalised and fitted to a Boltzmann equation:

$G = G_{max} / (1 + \exp (V_{1/2} - V_m) / k))$, where G_{max} is the maximum conductance, $V_{1/2}$ is the voltage at which the channels are half activated/inactivated, V_m is the membrane voltage and k is the slope factor.

Recovery from inactivation data ($I_t / I_{t=0}$) were normalised, plotted against recovery time (Δt) and fitted to a single exponential function:

$\tau = A_1 + A_2 \exp (-t / t_0)$, where A_1 and A_2 are the coefficients of decay of the time constant (τ), t is time and t_0 is a time constant describing the time dependence of τ.

The time course of inactivation was fitted to a double exponential function:

$I = A_f \exp (-t / \tau_f) + A_s \exp (-t / \tau_s) + C$, where A_f and A_s are maximal amplitudes of the slow and fast components of the current, τ_f and τ_s are the fast and slow decay time constants and C is the asymptote.

2.6 Statistical analysis

Data are presented as mean and SEM unless stated otherwise. Statistical analysis was performed using GraphPad Prism 8.4.0. Pairwise statistical significance was determined with Student's paired *t*-tests. Multiple comparisons were made using ANOVA and Tukey post-hoc tests, unless stated otherwise. Results were considered significant at $P < 0.05$.

3 Results

3.1 Effect of eslicarbazepine acetate and S-licarbazepine on transient and persistent Na^+ current

Several studies have clearly established the inhibition of neuronal VGSCs ($Na_v1.1$, $Na_v1.2$, $Na_v1.3$, $Na_v1.6$, $Na_v1.7$ and $Na_v1.8$) by ESL and its active metabolite S-Lic (10, 20, 24, 44). Given that ESL prolongs the PR interval (27), potentially via inhibiting the cardiac $Na_v1.5$ isoform, together with the potential interest in inhibiting $Na_v1.5$ in carcinoma cells to reduce invasion and metastasis (33, 34, 45-50), it is also relevant to evaluate the electrophysiological effects of ESL and S-Lic on this isoform. We therefore evaluated the effect of both compounds on $Na_v1.5$ current properties using whole-cell patch clamp recording, employing a two-pronged approach: (1) recording $Na_v1.5$ currents

157 endogenously expressed in the MDA-MB-231 breast cancer cell line (29, 30, 51), and (2) recording
158 from $Na_v1.5$ stably over-expressed in HEK-293 cells (HEK-$Na_v1.5$) (52).

159 Initially, we evaluated the effect of both compounds on the size of the peak Na^+ current in MDA-
160 MB-231 cells. Na^+ currents were elicited by depolarising the membrane potential (V_m) to -10 mV
161 from a holding potential (V_h) of -120 mV or -80 mV. Application of the prodrug ESL (300 µM)
162 reversibly inhibited the transient Na^+ current by 49.6 ± 3.2 % when the V_h was -120 mV ($P < 0.001$;
163 n = 13; ANOVA + Tukey test; Figure 2Ai, Bi). When V_h was set to -80 mV, ESL reversibly inhibited
164 the transient Na^+ current by 79.5 ± 4.5 % ($P < 0.001$; n = 12; ANOVA + Tukey test; Figure 2Aii,
165 Bii). We next assessed the effect of ESL in HEK-$Na_v1.5$ cells. Application of ESL inhibited $Na_v1.5$
166 current by 74.7 ± 4.3 % when V_h was -120 mV ($P < 0.001$; n = 14; Figure 2Ci, Di) and by 90.5 ± 2.8
167 % when V_h was -80 mV ($P < 0.001$; n = 14; Figure 2Cii, Dii). However, the inhibition was only
168 partially reversible ($P < 0.001$; n = 14; Figure 2C, D). Together, these data suggest that ESL
169 preferentially inhibited $Na_v1.5$ in the open or inactivated state, since the current inhibition was
170 greater at more depolarised V_h.

171 We next tested the effect of the active metabolite S-Lic. S-Lic (300 µM) inhibited the transient Na^+
172 current in MDA-MB-231 cells by 44.4 ± 6.1 % when the V_h was -120 mV ($P < 0.001$; n = 9;
173 ANOVA + Tukey test; Figure 3Ai, Bi). When V_h was set to -80 mV, S-Lic (300 µM) inhibited the
174 transient Na^+ current by 73.6 ± 4.1 % ($P < 0.001$; n = 10; ANOVA + Tukey test; Figure 3Aii, Bii).
175 However, the inhibition caused by S-Lic was only partially reversible ($P < 0.05$; n = 10; ANOVA +
176 Tukey test; Figure 3A, B). In HEK-$Na_v1.5$ cells, S-Lic inhibited $Na_v1.5$ current by 46.4 ± 3.93 %
177 when V_h was -120 mV ($P < 0.001$; n = 14; ANOVA + Tukey test; Figure 3Ci, Di) and by 74.0 ± 4.2
178 % when V_h was -80 mV ($P < 0.001$; n = 14; ANOVA + Tukey test; Figure 3Cii, Dii). Furthermore,
179 the inhibition in HEK-$Na_v1.5$ cells was not reversible over the duration of the experiment. Together,
180 these data show that channel inhibition by S-Lic was also more effective at more depolarised V_h.
181 However, unlike ESL, channel blockade by S-Lic persisted after washout, suggesting higher target
182 binding affinity for the active metabolite.

183 We also assessed the effect of both compounds on the persistent Na^+ current measured 20-25 ms after
184 depolarisation to -10 mV from -120 mV. In MDA-MB-231 cells, ESL inhibited the persistent Na^+
185 current from -0.12 ± 0.06 pA/pF to 0.03 ± 0.08 pA/pF although the reduction was not statistically
186 significant ($P = 0.07$; n = 13; paired t test; Table 1). In HEK-$Na_v1.5$ cells, ESL inhibited persistent
187 current from -0.61 ± 0.15 pA/pF to -0.55 ± 0.2 pA/pF ($P < 0.01$; n = 14; paired t test; Table 1). S-Lic
188 inhibited the persistent Na^+ current in MDA-MB-231 cells from -1.3 ± 0.4 pA/pF to -0.6 ± 0.2 pA/pF
189 ($P < 0.05$; n =9; paired t test; Table 2). In HEK-$Na_v1.5$ cells, S-Lic inhibited persistent current from -
190 0.9 ± 0.2 pA/pF to -0.5 ± 0.2 pA/pF ($P < 0.05$; n = 14; Table 2). In summary, both ESL and S-Lic
191 also inhibited the persistent Na^+ current.

192 **3.2 Effect of eslicarbazepine acetate and S-licarbazepine on voltage dependence of activation**
193 **and inactivation**

194 We next investigated the effect of ESL (300 µM) and S-Lic (300 µM) on the I-V relationship in
195 MDA-MB-231 and HEK-$Na_v1.5$ cells. A V_h of -120 mV was used for subsequent analyses to ensure
196 that the elicited currents were sufficiently large for analysis of kinetics and voltage dependence,
197 particularly for MDA-MB-231 cells, which display smaller peak Na^+ currents (Tables 1, 2). Neither
198 ESL nor S-Lic had any effect on the threshold voltage for activation (Figure 4A-D; Tables 1, 2). ESL
199 also had no effect on the voltage at current peak in either cell line (Figure 4A-D; Tables 1, 2).
200 Although S-Lic had no effect on voltage at current peak in MDA-MB-231 cells, it significantly

hyperpolarised in HEK-Nav1.5 cells from -18.0 ± 4.2 mV to -30.0 ± 5.5 mV ($P < 0.001$; n = 9; paired t test; Figure 4A-D; Tables 1, 2).

ESL had no significant effect on the half-activation voltage (V½) or slope factor (k) for activation in MDA-MB-231 cells (Figure 5A; Table 1). The activation k and V½ in HEK-$Na_v1.5$ cells were also unchanged (Figure 5B; Table 1). S-Lic also had no significant effect on the activation V½ or k in MDA-MB-231 cells (Figure 5C; Table 2). However, the V½ of activation in HEK-$Na_v1.5$ cells was significantly hyperpolarised from -32.8 ± 3.1 mV to -40.5 ± 3.4 mV ($P < 0.01$; n = 9; paired t test; Figure 5D; Table 2) and k changed from 5.9 ± 0.9 mV to 4.5 ± 1.1 mV ($P < 0.05$; n = 9; paired t test; Figure 5D; Table 2).

As regards steady-state inactivation, in MDA-MB-231 cells, ESL significantly hyperpolarised the inactivation V½ from -80.6 ± 0.7 mV to -86.7 ± 1.2 mV ($P < 0.001$; n = 13; paired t test) without affecting inactivation k (Figure 5A; Table 1). ESL also hyperpolarised the inactivation V½ in HEK-$Na_v1.5$ cells from -78.2 ± 2.5 mV to -88.3 ± 2.7 mV ($P < 0.001$; n = 10; paired t test), and changed the inactivation k from -6.9 ± 0.4 mV to -9.8 ± 0.7 mV ($P < 0.001$; n = 10; paired t test; Figure 5B; Table 1). S-Lic also significantly hyperpolarised the inactivation V½ in MDA-MB-231 cells from -71.8 ± 2.5 mV to -76.8 ± 2.2 mV ($P < 0.05$; n = 7; paired t test) without affecting inactivation k (Figure 5C; Table 2). However, the inactivation V½ in HEK-$Na_v1.5$ cells was not significantly altered by S-Lic, although the inactivation k significantly changed from -6.5 ± 0.4 mV to -8.1 ± 0.5 mV ($P < 0.05$; n = 9; paired t test; Figure 5D; Table 2). In summary, both ESL and S-Lic affected various aspects of the voltage dependence characteristics of $Na_v1.5$ in MDA-MB-231 and HEK-$Na_v1.5$ cells, predominantly hyperpolarising the voltage dependence of inactivation.

3.3 Effect of eslicarbazepine acetate and S-licarbazepine on activation and inactivation kinetics

We next studied the effect of both compounds on kinetics of activation and inactivation. In MDA-MB-231 cells, ESL significantly accelerated the time to peak current (T_p) upon depolarisation to -10 mV from 2.1 ± 0.2 ms to 1.9 ± 0.2 ms ($P < 0.01$; n = 13; paired t test; Table 1). However, in HEK-$Na_v1.5$ cells, ESL significantly slowed T_p from 1.4 ± 0.1 ms to 1.5 ± 0.2 ms ($P < 0.001$; n = 14; paired t test; Table 1). S-Lic had no significant effect on T_p in MDA-MB-231 cells but significantly slowed T_p in HEK-$Na_v1.5$ cells from 1.8 ± 0.5 ms to 2.3 ± 0.6 ms ($P < 0.01$; n = 14; paired t test; Table 1).

To study effects on inactivation kinetics, the current decay following depolarisation from -120 mV to -10 mV was fitted to a double exponential function to derive fast and slow time constants of inactivation (τ_f and τ_s). Neither ESL nor S-Lic had any significant effect on τ_f or τ_s in MDA-MB-231 cells (Tables 1, 2). However, in HEK-$Na_v1.5$ cells, ESL significantly slowed τ_f from 0.9 ± 0.1 ms to 1.2 ± 0.1 ms ($P < 0.001$; n = 14; paired t test; Table 1) and slowed τ_s from 6.6 ± 0.8 ms to 20.8 ± 8.4 ms, although this was not statistically significant. S-Lic significantly slowed τ_f from 1.0 ± 0.0 ms to 1.3 ± 0.1 ms ($P < 0.001$; n = 14; paired t test; Table 2) and τ_s from 6.3 ± 0.5 ms to 7.3 ± 0.5 ms ($P < 0.05$; n = 14; paired t test; Table 2). In summary, both ESL and S-Lic elicited various effects on kinetics in MDA-MB-231 and HEK-$Na_v1.5$ cells, predominantly slowing activation and inactivation.

3.4 Use-dependent effect of eslicarbazepine acetate and S-licarbazepine on $Na_v1.5$

To study use-dependent block of Na^+ current by ESL and S-Lic, we ran a protocol where cells were subjected to repeated depolarisations from -120 mV to 0 mV, at a frequency of 50 Hz. In MDA-MB-231 cells, this depolarisation train caused a rapid decrease in current size, which reached a plateau of

244 90.1 % of the initial current after the first pulse (Figure 5A). In the presence of ESL, the decrease in
245 current reached a plateau of 83.7 % after the third pulse (Figure 6A), indicating use-dependent block
246 of the channel. S-Lic had a similar but less obvious effect where the current declined to 85.1 % in the
247 presence of S-Lic, compared to 87.5 % without drug (Figure 6B).

248 Use-dependent block was easier to study in HEK-$Na_v1.5$ cells due to the larger Na^+ current. In these
249 cells, ESL increased the reduction in current amplitude to 71.6 % of the initial current, compared to
250 88.9 % without drug (Figure 6C). S-Lic also increased the reduction in current amplitude to 76.1 %
251 of the initial current, compared to 85.7 % without drug. Together, these results indicate that both ESL
252 and S-Lic cause use-dependent block of $Na_v1.5$.

253 **3.5 Effect of eslicarbazepine acetate and S-licarbazepine on recovery from fast inactivation**

254 To investigate the effect of ESL and S-Lic on channel recovery from fast inactivation, we subjected
255 cells to two depolarisations from V_h of -120 mV to 0 mV, changing the interval between these in
256 which the channels were held at -120 mV to facilitate recovery. Significance was determined by
257 fitting a single exponential curve to the normalised current/time relationship and calculating the time
258 constant (τ_r). In MDA-MB-231 cells, ESL significantly slowed τ_r from 6.0 ± 0.5 ms to 8.7 ± 0.7 ms
259 ($P < 0.05$; n = 10; paired t test; Figure 7A, Table 1). Similarly, in HEK-$Na_v1.5$ cells, ESL
260 significantly slowed τ_r from 4.5 ± 0.4 ms to 7.1 ± 0.6 ms ($P < 0.001$; n = 10; paired t test; Figure 7B,
261 Table 1). S-Lic also significantly slowed τ_r in MDA-MB-231 cells from 6.8 ± 0.4 ms to 13.5 ± 1.1
262 ms ($P < 0.01$; n = 7; paired t test; Figure 7C, Table 2). Finally, S-Lic also significantly slowed τ_r in
263 HEK-$Na_v1.5$ cells from 5.7 ± 0.7 ms to 8.0 ± 1.2 ms ($P < 0.01$; n = 10; paired t test; Figure 7D, Table
264 2). In summary, both ESL and S-Lic slowed recovery from fast inactivation of $Na_v1.5$.

265 **4 Discussion**

266 In this study, we have shown that ESL and its active metabolite S-Lic (both at 300 μM) inhibit the
267 transient and persistent components of Na^+ current carried by $Na_v1.5$. We show broadly similar
268 effects in MDA-MB-231 cells, which express endogenous $Na_v1.5$ (29, 30, 51), and in HEK-293 cells
269 over-expressing $Na_v1.5$. Notably, both compounds were more effective when V_h was set to -80 mV
270 than at -120 mV, suggestive of depolarised state-dependent binding. In addition, the inhibitory effect
271 of ESL was reversible whereas inhibition by S-Lic was not. As regards voltage-dependence, both
272 ESL and S-Lic shifted activation and steady-state inactivation curves, to varying extents in the two
273 cell lines, in the direction of more negative voltages. ESL and S-Lic had various effects on activation
274 and inactivation kinetics, generally slowing the rate of inactivation. Both ESL and S-Lic also caused
275 use-dependent block of $Na_v1.5$, although the effect was more obvious in HEK-$Na_v1.5$ cells due to the
276 larger Na^+ current. Finally, recovery from fast inactivation of $Na_v1.5$ was significantly slowed by
277 both ESL and S-Lic.

278 To our knowledge, this is the first time that the effects of ESL and S-Lic have specifically been tested
279 on the $Na_v1.5$ isoform. A strength of this study is that both the prodrug (ESL) and the active
280 metabolite (S-Lic) were tested using two independent cell lines, one endogenously expressing
281 $Na_v1.5$, the other stably over-expressing $Na_v1.5$. Interestingly, MDA-MB-231 cells predominantly
282 express the developmentally regulated 'neonatal' $Na_v1.5$ splice variant, which differs from the 'adult'
283 variant over-expressed in the HEK-$Na_v1.5$ cells by seven amino acids located in the extracellular
284 linker between transmembrane segments 3 and 4 of domain 1 (30, 45, 51). Notably, however, there
285 were no consistent differences in effect of either ESL or S-Lic between the MDA-MB-231 and HEK-
286 $Na_v1.5$ cells, suggesting that the neonatal vs. adult splicing event does not impact on sensitivity of

287 $Na_v1.5$ to these compounds. This finding contrasts another report showing different sensitivity of the
288 neonatal and adult $Na_v1.5$ splice variants to the amide local anaesthetics lidocaine and
289 levobupivacaine (49). Our findings suggest that the inhibitory effect of S-Lic on $Na_v1.5$ is less
290 reversible than that of ESL. This may be explained by the differing chemical structures of the two
291 molecules possibly enabling S-Lic to bind the target with higher affinity than ESL. Most VGSC-
292 targeting anticonvulsants, including phenytoin, lamotrigine and carbamazepine, block the pore by
293 binding via aromatic-aromatic interaction to a tyrosine and phenylalanine located in the S6 helix of
294 domain 4 (53). However, S-Lic has been proposed to bind to a different site given that it was found
295 to block the pore predominantly during slow inactivation (10). Alternatively, the hydroxyl group
296 present on S-Lic (but not ESL) may become deprotonated, potentially trapping it in the cytoplasm.

297 This study used a single concentration for both compounds (300 μM) and the findings presented here
298 broadly agree with *in vitro* concentrations used elsewhere to study effects of ESL and S-Lic on Na^+
299 currents. For example, using a V_h of -80 mV, 300 μM ESL was shown to inhibit peak Na^+ current by
300 50 % in N1E-115 neuroblastoma cells expressing $Na_v1.1$, $Na_v1.2$, $Na_v1.3$, $Na_v1.6$ and $Na_v1.7$ (20). S-
301 Lic (250 μM) also blocks peak Na^+ current by ~50 % in the same cell line (10). In addition, S-Lic
302 (300 μM) reduces persistent Na^+ current by ~25 % in acutely isolated murine hippocampal CA1
303 neurons expressing $Na_v1.1$, $Na_v1.2$ and $Na_v1.6$ (21-24). Similar to the present study, ESL was shown
304 to hyperpolarise the voltage-dependence of steady-state inactivation in N1E-115 cells (20). On the
305 other hand, similar to our finding in HEK-$Na_v1.5$ cells, S-Lic has no effect on steady-state
306 inactivation in H1E-115 cells (10). Again, in agreement with our own findings for $Na_v1.5$, S-Lic
307 slows recovery from inactivation and causes use-dependent inhibition in H1E-115 cells (10).
308 Together, these observations suggest that the sensitivity of $Na_v1.5$ to ESL and S-Lic is broadly
309 similar to that reported for neuronal VGSCs. In support of this, $Na_v1.5$ shares the same conserved
310 residues proposed for $Na_v1.2$ to interact with ESL (Figure 8) (54). Notably, the concentration used in
311 this study is high compared with concentrations achieved in clinical use (e.g. ESL 1200 mg QD gives
312 a peak plasma concentration of ~90 μM) (10). However, it has been argued that the relatively high
313 concentrations required for channel inhibition *in vitro* are clinically relevant given that S-Lic has a
314 high (50:1) lipid:water partition co-efficient and thus would be expected to reside predominantly in
315 the tissue membrane fraction *in vivo* (15).

316 The data presented here raise several implications for clinicians. The observed tonic and use-
317 dependent inhibition of $Na_v1.5$ is worthy of note when considering cardiac function in patients
318 receiving ESL (13). Although the QT interval remains unchanged for individuals on ESL treatment,
319 prolongation of the PR interval has been observed (27). Further work is required to establish whether
320 the basis for this PR prolongation is indeed via $Na_v1.5$ inhibition. In addition, it would be of interest
321 to investigate the efficacy of ESL and S-Lic in the context of heritable arrhythmogenic mutations in
322 *SCN5A*, as well as the possible involvement of the β subunits (24, 26, 55, 56). The findings presented
323 here are also relevant in the context of $Na_v1.5$ expression in carcinoma cells (57). Given that cancer
324 cells have a relatively depolarised V_m, it is likely that $Na_v1.5$ is mainly in the inactivated state with
325 the persistent Na^+ current being functionally predominant (35, 40, 58, 59). Increasing evidence
326 suggests that persistent Na^+ current carried by $Na_v1.5$ in cancer cells contributes to invasion and
327 several studies have shown that other VGSC inhibitors reduce metastasis in preclinical models (29-
328 35, 60). Thus, use-dependent inhibition by ESL would ensure that channels in malignant cells are
329 particularly targeted, raising the possibility that it could be used as an anti-metastatic agent (47). This
330 study therefore paves the way for future investigations into ESL and S-Lic as potential invasion
331 inhibitors.

332 **5 Author Contributions**

TL, SC and WB contributed to the conception and design of the work. TL, LB and WB contributed to acquisition, analysis, and interpretation of data for the work. TL, SC and WB contributed to drafting the work and revising it critically for important intellectual content. All authors approved the final version of the manuscript.

6 Abbreviations

ESL, eslicarbazepine acetate; HEK-$Na_v1.5$, HEK-293 cells stably expressing $Na_v1.5$; I-V, current-voltage; k, slope factor; PSS, physiological saline solution; S-Lic, S-licarbazepine, T_p: time to peak current; τ_f: fast time constant of inactivation; τ_s: slow time constant of inactivation; τ_r: time constant of recovery from inactivation; VGSC, voltage-gated Na^+ channel; V_m, membrane potential; V_h, holding potential; V_{peak}: voltage at which current was maximal;V_{rev}, reversal potential; V_{thres}: threshold voltage for activation; $V_{1/2}$, half-activation voltage.

7 Acknowledgements

This work was supported by Cancer Research UK (A25922) and Breast Cancer Now (2015NovPhD572).

8 Conflict of interest statement

The authors declare that the research was conducted in the absence of any commercial or financial relationships that could be construed as a potential conflict of interest.

9 Data availability statement

The datasets used and/or analysed during the current study are available from the corresponding author on reasonable request.

10 References

1. Almeida L, Soares-da-Silva P. Eslicarbazepine acetate (BIA 2-093). Neurotherapeutics. 2007;4(1):88-96.

2. Sperling MR, Abou-Khalil B, Harvey J, Rogin JB, Biraben A, Galimberti CA, et al. Eslicarbazepine acetate as adjunctive therapy in patients with uncontrolled partial-onset seizures: Results of a phase III, double-blind, randomized, placebo-controlled trial. Epilepsia. 2015;56(2):244-53.

3. Almeida L, Falcao A, Maia J, Mazur D, Gellert M, Soares-da-Silva P. Single-dose and steady-state pharmacokinetics of eslicarbazepine acetate (BIA 2-093) in healthy elderly and young subjects. J Clin Pharmacol. 2005;45(9):1062-6.

4. Almeida L, Minciu I, Nunes T, Butoianu N, Falcão A, Magureanu S-A, et al. Pharmacokinetics, Efficacy, and Tolerability of Eslicarbazepine Acetate in Children and Adolescents With Epilepsy. The Journal of Clinical Pharmacology. 2008;48(8):966-77.

5. Perucca E, Elger C, Halász P, Falcão A, Almeida L, Soares-da-Silva P. Pharmacokinetics of eslicarbazepine acetate at steady-state in adults with partial-onset seizures. Epilepsy Res. 2011;96(1):132-9.

369 6. Potschka H, Soerensen J, Pekcec A, Loureiro A, Soares-da-Silva P. Effect of eslicarbazepine
370 acetate in the corneal kindling progression and the amygdala kindling model of temporal lobe
371 epilepsy. Epilepsy Res. 2014;108(2):212-22.

372 7. Sierra-Paredes G, Loureiro AI, Wright LC, Sierra-Marcuño G, Soares-da-Silva P. Effects of
373 eslicarbazepine acetate on acute and chronic latrunculin A-induced seizures and extracellular amino
374 acid levels in the mouse hippocampus. BMC Neurosci. 2014;15(1):134.

375 8. Alves G, Figueiredo I, Falcao A, Castel-Branco M, Caramona M, Soares-Da-Silva P.
376 Stereoselective disposition of S- and R-licarbazepine in mice. Chirality. 2008;20(6):796-804.

377 9. Brady K, Hebeisen S, Konrad D, Soares-da-Silva P. The effects of eslicarbazepine, R-
378 licarbazepine, oxcarbazepine and carbamazepine on ion transmission Cav3.2 channels. Epilepsia.
379 2011;52:260.

380 10. Hebeisen S, Pires N, Loureiro AI, Bonifacio MJ, Palma N, Whyment A, et al. Eslicarbazepine
381 and the enhancement of slow inactivation of voltage-gated sodium channels: a comparison with
382 carbamazepine, oxcarbazepine and lacosamide. Neuropharmacology. 2015;89:122-35.

383 11. Brown ME, El-Mallakh RS. Role of eslicarbazepine in the treatment of epilepsy in adult
384 patients with partial-onset seizures. Ther Clin Risk Manag. 2010;6:103-9.

385 12. Galiana GL, Gauthier AC, Mattson RH. Eslicarbazepine Acetate: A New Improvement on a
386 Classic Drug Family for the Treatment of Partial-Onset Seizures. Drugs R D. 2017;17(3):329-39.

387 13. Zaccara G, Giovannelli F, Cincotta M, Carelli A, Verrotti A. Clinical utility of
388 eslicarbazepine: current evidence. Drug Des Devel Ther. 2015;9:781-9.

389 14. Falcao A, Fuseau E, Nunes T, Almeida L, Soares-da-Silva P. Pharmacokinetics, drug
390 interactions and exposure-response relationship of eslicarbazepine acetate in adult patients with
391 partial-onset seizures: population pharmacokinetic and pharmacokinetic/pharmacodynamic analyses.
392 CNS Drugs. 2012;26(1):79-91.

393 15. Bialer M, Soares-da-Silva P. Pharmacokinetics and drug interactions of eslicarbazepine
394 acetate. Epilepsia. 2012;53(6):935-46.

395 16. Catterall WA. Structure and function of voltage-gated sodium channels at atomic resolution.
396 Exp Physiol. 2014;99(1):35-51.

397 17. Goldin AL, Barchi RL, Caldwell JH, Hofmann F, Howe JR, Hunter JC, et al. Nomenclature
398 of voltage-gated sodium channels. Neuron. 2000;28:365-8.

399 18. Brackenbury WJ, Isom LL. Na Channel beta Subunits: Overachievers of the Ion Channel
400 Family. Front Pharmacol. 2011;2:53.

401 19. Van Wart A, Matthews G. Impaired firing and cell-specific compensation in neurons lacking
402 nav1.6 sodium channels. J Neurosci. 2006;26(27):7172-80.

403 20. Bonifacio MJ, Sheridan RD, Parada A, Cunha RA, Patmore L, Soares-da-Silva P. Interaction
404 of the novel anticonvulsant, BIA 2-093, with voltage-gated sodium channels: comparison with
405 carbamazepine. Epilepsia. 2001;42(5):600-8.

406 21. Royeck M, Horstmann MT, Remy S, Reitze M, Yaari Y, Beck H. Role of axonal NaV1.6
407 sodium channels in action potential initiation of CA1 pyramidal neurons. J Neurophysiol.
408 2008;100(4):2361-80.

409 22. Yu FH, Mantegazza M, Westenbroek RE, Robbins CA, Kalume F, Burton KA, et al. Reduced
410 sodium current in GABAergic interneurons in a mouse model of severe myoclonic epilepsy in
411 infancy. Nat Neurosci. 2006;9(9):1142-9.

412 23. Westenbroek RE, Merrick DK, Catterall WA. Differential subcellular localization of the RI
413 and RII Na+ channel subtypes in central neurons. Neuron. 1989;3(6):695-704.

414 24. Doeser A, Soares-da-Silva P, Beck H, Uebachs M. The effects of eslicarbazepine on
415 persistent Na(+) current and the role of the Na(+) channel beta subunits. Epilepsy Res.
416 2014;108(2):202-11.

417 25. Saint DA. The cardiac persistent sodium current: an appealing therapeutic target? Br J
418 Pharmacol. 2008;153(6):1133-42.

419 26. Uebachs M, Opitz T, Royeck M, Dickhof G, Horstmann MT, Isom LL, et al. Efficacy loss of
420 the anticonvulsant carbamazepine in mice lacking sodium channel beta subunits via paradoxical
421 effects on persistent sodium currents. J Neurosci. 2010;30(25):8489-501.

422 27. Vaz-Da-Silva M, Nunes T, Almeida L, Gutierrez MJ, Litwin JS, Soares-Da-Silva P.
423 Evaluation of Eslicarbazepine acetate on cardiac repolarization in a thorough QT/QTc study. J Clin
424 Pharmacol. 2012;52(2):222-33.

425 28. George AL, Jr. Inherited disorders of voltage-gated sodium channels. J Clin Invest.
426 2005;115(8):1990-9.

427 29. Roger S, Besson P, Le Guennec JY. Involvement of a novel fast inward sodium current in the
428 invasion capacity of a breast cancer cell line. Biochim Biophys Acta. 2003;1616(2):107-11.

429 30. Fraser SP, Diss JK, Chioni AM, Mycielska ME, Pan H, Yamaci RF, et al. Voltage-gated
430 sodium channel expression and potentiation of human breast cancer metastasis. Clin Cancer Res.
431 2005;11(15):5381-9.

432 31. House CD, Vaske CJ, Schwartz AM, Obias V, Frank B, Luu T, et al. Voltage-gated Na+
433 channel SCN5A is a key regulator of a gene transcriptional network that controls colon cancer
434 invasion. Cancer Res. 2010;70(17):6957-67.

435 32. Nelson M, Yang M, Millican-Slater R, Brackenbury WJ. Nav1.5 regulates breast tumor
436 growth and metastatic dissemination in vivo. Oncotarget. 2015;6(32):32914-29.

437 33. Nelson M, Yang M, Dowle AA, Thomas JR, Brackenbury WJ. The sodium channel-blocking
438 antiepileptic drug phenytoin inhibits breast tumour growth and metastasis. Mol Cancer.
439 2015;14(1):13.

440 34. Driffort V, Gillet L, Bon E, Marionneau-Lambot S, Oullier T, Joulin V, et al. Ranolazine
441 inhibits NaV1.5-mediated breast cancer cell invasiveness and lung colonization. Mol Cancer.
442 2014;13(1):264.

443 35. Yang M, Kozminski DJ, Wold LA, Modak R, Calhoun JD, Isom LL, et al. Therapeutic
444 potential for phenytoin: targeting Na(v)1.5 sodium channels to reduce migration and invasion in
445 metastatic breast cancer. Breast Cancer Res Treat. 2012;134(2):603-15.

446 36. Simon A, Yang M, Marrison JL, James AD, Hunt MJ, O'Toole PJ, et al. Metastatic breast
447 cancer cells induce altered microglial morphology and electrical excitability in vivo. J
448 Neuroinflammation. 2020;17(1):87.

449 37. Masters JR, Thomson JA, Daly-Burns B, Reid YA, Dirks WG, Packer P, et al. Short tandem
450 repeat profiling provides an international reference standard for human cell lines. Proc Natl Acad Sci
451 U S A. 2001;98(14):8012-7.

452 38. Uphoff CC, Gignac SM, Drexler HG. Mycoplasma contamination in human leukemia cell
453 lines. I. Comparison of various detection methods. J Immunol Methods. 1992;149(1):43-53.

454 39. Chioni AM, Brackenbury WJ, Calhoun JD, Isom LL, Djamgoz MB. A novel adhesion
455 molecule in human breast cancer cells: voltage-gated Na+ channel beta1 subunit. Int J Biochem Cell
456 Biol. 2009;41(5):1216-27.

457 40. Yang M, James AD, Suman R, Kasprowicz R, Nelson M, O'Toole PJ, et al. Voltage-
458 dependent activation of Rac1 by Nav 1.5 channels promotes cell migration. J Cell Physiol.
459 2020;235(4):3950-72.

460 41. Thurber AE, Nelson M, Frost CL, Levin M, Brackenbury WJ, Kaplan DL. IK channel
461 activation increases tumor growth and induces differential behavioral responses in two breast
462 epithelial cell lines. Oncotarget. 2017;8(26):42382-97.

463 42. Brackenbury WJ, Djamgoz MB. Activity-dependent regulation of voltage-gated Na^+ channel
464 expression in Mat-LyLu rat prostate cancer cell line. J Physiol. 2006;573(Pt 2):343-56.

465 43. Armstrong CM, Bezanilla F. Inactivation of the sodium channel. II. Gating current
466 experiments. J Gen Physiol. 1977;70(5):567-90.

467 44. Soares-da-Silva P, Pires N, Bonifácio MJ, Loureiro AI, Palma N, Wright LC. Eslicarbazepine
468 acetate for the treatment of focal epilepsy: an update on its proposed mechanisms of action.
469 Pharmacol Res Perspect. 2015;3(2).

470 45. Djamgoz MBA, Fraser SP, Brackenbury WJ. In Vivo Evidence for Voltage-Gated Sodium
471 Channel Expression in Carcinomas and Potentiation of Metastasis. Cancers (Basel). 2019;11(11).

472 46. Fairhurst C, Watt I, Martin F, Bland M, Brackenbury WJ. Sodium channel-inhibiting drugs
473 and survival of breast, colon and prostate cancer: a population-based study. Sci Rep. 2015;5:16758.

474 47. Martin F, Ufodiama C, Watt I, Bland M, Brackenbury WJ. Therapeutic value of voltage-gated
475 sodium channel inhibitors in breast, colorectal and prostate cancer: a systematic review. Front
476 Pharmacol. 2015;6:273.

477 48. Baptista-Hon DT, Robertson FM, Robertson GB, Owen SJ, Rogers GW, Lydon EL, et al.
478 Potent inhibition by ropivacaine of metastatic colon cancer SW620 cell invasion and NaV1.5 channel
479 function. Br J Anaesth. 2014;113 Suppl 1:i39-i48.

480 49. Elajnaf T, Baptista-Hon DT, Hales TG. Potent Inactivation-Dependent Inhibition of Adult
481 and Neonatal NaV1.5 Channels by Lidocaine and Levobupivacaine. Anesth Analg. 2018;127(3):650-
482 60.

483 50. Dutta S, Lopez Charcas O, Tanner S, Gradek F, Driffort V, Roger S, et al. Discovery and
484 evaluation of nNav1.5 sodium channel blockers with potent cell invasion inhibitory activity in breast
485 cancer cells. Bioorg Med Chem. 2018;26(9):2428-36.

486 51. Brackenbury WJ, Chioni AM, Diss JK, Djamgoz MB. The neonatal splice variant of Nav1.5
487 potentiates in vitro metastatic behaviour of MDA-MB-231 human breast cancer cells. Breast Cancer
488 Res Treat. 2007;101(2):149-60.

489 52. Patino GA, Brackenbury WJ, Bao YY, Lopez-Santiago LF, O'Malley HA, Chen CL, et al.
490 Voltage-Gated Na+ Channel beta 1B: A Secreted Cell Adhesion Molecule Involved in Human
491 Epilepsy. J Neurosci. 2011;31(41):14577-91.

492 53. Lipkind GM, Fozzard HA. Molecular model of anticonvulsant drug binding to the voltage-
493 gated sodium channel inner pore. Mol Pharmacol. 2010;78(4):631-8.

494 54. Shaikh S, Rizvi SM, Hameed N, Biswas D, Khan M, Shakil S, et al. Aptiom (eslicarbazepine
495 acetate) as a dual inhibitor of beta-secretase and voltage-gated sodium channel: advancement in
496 Alzheimer's disease-epilepsy linkage via an enzoinformatics study. CNS Neurol Disord Drug
497 Targets. 2014;13(7):1258-62.

498 55. Brackenbury WJ, Isom LL. Voltage-gated Na+ channels: potential for beta subunits as
499 therapeutic targets. Expert Opin Ther Targets. 2008;12(9):1191-203.

500 56. Rivaud MR, Delmar M, Remme CA. Heritable arrhythmia syndromes associated with
501 abnormal cardiac sodium channel function: ionic and non-ionic mechanisms. Cardiovasc Res. 2020.

502 57. Fraser SP, Ozerlat-Gunduz I, Brackenbury WJ, Fitzgerald EM, Campbell TM, Coombes RC,
503 et al. Regulation of voltage-gated sodium channel expression in cancer: hormones, growth factors
504 and auto-regulation. Philos Trans R Soc Lond B Biol Sci. 2014;369(1638):20130105.

505 58. Yang M, Brackenbury WJ. Membrane potential and cancer progression. Front Physiol.
506 2013;4:185.

507 59. Patel F, Brackenbury WJ. Dual roles of voltage-gated sodium channels in development and
508 cancer. Int J Dev Biol. 2015;59:357-66.

509 60. Besson P, Driffort V, Bon E, Gradek F, Chevalier S, Roger S. How do voltage-gated sodium
510 channels enhance migration and invasiveness in cancer cells? Biochim Biophys Acta. 2015;1848(10
511 Pt B):2493-501.

512

513 **10.1 Figure legends**

514 **Figure 1.** Chemical structures of eslicarbazepine acetate and S-licarbazepine. (A) eslicarbazepine
515 acetate; (9S)-2-carbamoyl-2-azatricyclo[9.4.0.0^{3,8}]pentadeca-1(15),3,5,7,11,13-hexaen-9-yl acetate.
516 (B) S-licarbazepine; (10R)-10-hydroxy-2-azatricyclo[9.4.0.0^{3,8}]pentadeca-1(11),3,5,7,12,14-hexaene-
517 2-carboxamide. Structures were drawn using Chemspider software.

518 **Figure 2.** Effect of eslicarbazepine acetate on $Na_v1.5$ currents. (A) Na^+ currents in an MDA-MB-231
519 cell elicited by a depolarisation from (i) -120 mV and (ii) -80 mV to -10 mV in physiological saline
520 solution (PSS; black), eslicarbazepine acetate (ESL; 300 μM; red) and after washout (grey). (B)
521 Normalised Na^+ currents in MDA-MB-231 cells elicited by a depolarisation from (i) -120 mV and
522 (ii) -80 mV to -10 mV, in PSS, ESL (300 μM) and after washout. (C) Na^+ currents in a HEK-$Na_v1.5$
523 cell elicited by a depolarisation from (i) -120 mV and (ii) -80 mV to -10 mV in PSS (black), ESL
524 (300 μM; red) and after washout (grey). (D) Normalised Na^+ currents in HEK-$Na_v1.5$ cells elicited by
525 a depolarisation from (i) -120 mV and (ii) -80 mV to -10 mV, in PSS, ESL (300 μM) and after
526 washout. Results are mean + SEM. **$P \leq 0.01$; ***$P \leq 0.001$; one-way ANOVA with Tukey tests (n
527 = 12-14). NS, not significant.

528 **Figure 3.** Effect of S-licarbazepine on $Na_v1.5$ currents. (A) Na^+ currents in an MDA-MB-231 cell
529 elicited by a depolarisation from (i) -120 mV and (ii) -80 mV to -10 mV in physiological saline

530 solution (PSS; black), S-licarbazepine (S-Lic; 300 μM; red) and after washout (grey). (B) Normalised
531 Na^+ currents in MDA-MB-231 cells elicited by a depolarisation from (i) -120 mV and (ii) -80 mV to
532 -10 mV, in PSS, S-Lic (300 μM) and after washout. (C) Na^+ currents in a HEK-$Na_v1.5$ cell elicited
533 by a depolarisation from (i) -120 mV and (ii) -80 mV to -10 mV in PSS (black), S-Lic (300 μM; red)
534 and after washout (grey). (D) Normalised Na^+ currents in HEK-$Na_v1.5$ cells elicited by a
535 depolarisation from (i) -120 mV and (ii) -80 mV to -10 mV, in PSS, S-Lic (300 μM) and after
536 washout. Results are mean + SEM. *$P \leq 0.05$; ***$P \leq 0.001$; one-way ANOVA with Tukey tests (n =
537 9-13). NS, not significant.

538 **Figure 4.** Effect of eslicarbazepine acetate and S-licarbazepine on the current-voltage relationship.
539 (A) Current-voltage (I-V) plots of Na^+ currents in MDA-MB-231 cells in physiological saline
540 solution (PSS; black circles) and in eslicarbazepine acetate (ESL; 300 μM; red squares). (B) (I-V)
541 plots of Na^+ currents in HEK-$Na_v1.5$ cells in PSS (black circles) and ESL (300 μM; red squares). (C)
542 I-V plots of Na^+ currents in MDA-MB-231 cells in PSS (black circles) and S-licarbazepine (S-Lic;
543 300 μM; red squares). (D) I-V plots of Na^+ currents in HEK-$Na_v1.5$ cells in PSS (black circles) and
544 S-Lic (300 μM; red squares). Currents were elicited using 10 mV depolarising steps from -80 to +30
545 mV for 30 ms, from a holding potential of -120 mV. Results are mean ± SEM (n = 7-13).

546 **Figure 5.** Effect of eslicarbazepine acetate and S-licarbazepine on activation and steady-state
547 inactivation. (A) Activation and steady-state inactivation in MDA-MB-231 cells in physiological
548 saline solution (PSS; black circles) and in eslicarbazepine acetate (ESL; 300 μM; red squares). (B)
549 Activation and steady-state inactivation in HEK-$Na_v1.5$ cells in PSS (black circles) and ESL (300
550 μM; red squares). (C) Activation and steady-state inactivation in MDA-MB-231 cells in PSS (black
551 circles) and S-licarbazepine (S-Lic; 300 μM; red squares). (D) Activation and steady-state
552 inactivation in HEK-$Na_v1.5$ cells in PSS (black circles) and S-Lic (300 μM; red squares). For
553 activation, normalised conductance (G/G_{max}) was calculated from the current data and plotted as a
554 function of voltage. For steady-state inactivation, normalised current (I/I_{max}), elicited by 50 ms test
555 pulses at -10 mV following 250 ms conditioning voltage pulses between -120 mV and +30 mV,
556 applied from a holding potential of -120 mV, was plotted as a function of the prepulse voltage.
557 Results are mean ± SEM (n = 7-13). Activation and inactivation curves are fitted with Boltzmann
558 functions.

559 **Figure 6.** Use-dependent block by eslicarbazepine acetate and S-licarbazepine. (A) Rundown of Na^+
560 current in MDA-MB-231 cells in physiological saline solution (PSS; black circles) and in
561 eslicarbazepine acetate (ESL; 300 μM; red squares). (B) Rundown of Na^+ current in HEK-$Na_v1.5$
562 cells in PSS (black circles) and ESL (300 μM; red squares). (C) Rundown of Na^+ current in MDA-
563 MB-231 cells in PSS (black circles) and S-licarbazepine (S-Lic; 300 μM; red squares). (D) Rundown
564 of Na^+ current in HEK-$Na_v1.5$ cells in PSS (black circles) and S-Lic (300 μM; red squares). Currents
565 were elicited by 50 Hz pulse trains to 0 mV, applied from a holding potential of -120 mV, normalised
566 to the current evoked by the first pulse plotted as a function of the pulse number. Data are fitted with
567 single exponential functions. Results are mean ± SEM (n = 7-10).

568 **Figure 7.** Effect of eslicarbazepine acetate and S-licarbazepine on recovery from inactivation. (A)
569 Recovery from inactivation in MDA-MB-231 cells in physiological saline solution (PSS; black
570 circles) and in eslicarbazepine acetate (ESL; 300 μM; red squares). (B) Recovery from inactivation in
571 HEK-$Na_v1.5$ cells in PSS (black circles) and ESL (300 μM; red squares). (C) Recovery from
572 inactivation in MDA-MB-231 cells in PSS (black circles) and S-licarbazepine (S-Lic; 300 μM; red
573 squares). (D) Recovery from inactivation in HEK-$Na_v1.5$ cells in PSS (black circles) and S-Lic (300
574 μM; red squares). The fraction recovered (I_t/I_c) was determined by a 25 ms pulse to 0 mV (I_c),

575 followed by a recovery pulse to -120 mV for 1-500 ms, and a subsequent 25 ms test pulse to 0 mV
576 (I_t), applied from a holding potential of -120 mV, and plotted as a function of the recovery interval.
577 Data are fitted with single exponential functions which are statistically different between control and
578 drug treatments in all cases. Results are mean ± SEM (n = 7-10 cells).

579 **Figure 8.** Clustal alignment of amino acid sequences of $Na_v1.2$ (*SCN2A*) and $Na_v1.5$ (*SCN5A*). ESL
580 was proposed previously (54) to interact with the highlighted amino acids in $Na_v1.2$. An alignment of
581 $Na_v1.2$ (UniProtKB - Q99250 (SCN2A_HUMAN)) and $Na_v1.5$ (UniProtKB - Q14524
582 (SCN5A_HUMAN)) shows that the interacting amino acids highlighted in yellow are conserved
583 between the two isoforms (asterisks). Colon indicates conservation between groups of strongly
584 similar properties - scoring > 0.5 in the Gonnet PAM 250 matrix. Period indicates conservation
585 between groups of weakly similar properties - scoring ≤ 0.5 in the Gonnet PAM 250 matrix.

586 **Table 1.** Effect of eslicarbazepine acetate on Na^+ current characteristics in MDA-MB-231 and HEK-
587 $Na_v1.5$ cells.[1]

A. MDA-MB-231 cells			
Parameter	*Control*	*ESL*	*P value*
V_{thres} (mV)	-45.7 ± 1.7	-45.0 ± 1.4	0.58
V_{peak} (mV)	3.1 ± 2.1	-3.9 ± 2.7	0.056
Activation V½ (mV)	-19.3 ± 1.4	-22.0 ± 1.5	0.095
Activation k (mV)	10.6 ± 0.7	9.3 ± 0.8	0.076
Inactivation V½ (mV)	-80.6 ± 0.7	-86.7 ± 1.2	<0.001
Inactivation k (mV)	-4.8 ± 0.4	-7.4 ± 1.7	0.139
Peak current density at -10 mV (pA/pF)	-14.8 ± 3.9	-8.0 ± 2.5	<0.001
Persistent current density at -10 mV (pA/pF)	-0.12 ± 0.06	0.03 ± 0.08	0.068
T_p at -10 mV (ms)	2.1 ± 0.2	1.9 ± 0.2	<0.01
τ_f at -10 mV (ms)	1.3 ± 0.1	1.3 ± 0.2	0.954
τ_s at -10 mV) (ms)	10.0 ± 2.3	6.9 ± 2.0	0.289
τ_r (ms)	6.0 ± 0.5	8.7 ± 0.7	<0.05
B. HEK-$Na_v1.5$ cells			
Parameter	*Control*	*ESL*	*P value*
V_{thres} (mV)	-55.0 ± 1.7	-54.0 ± 2.2	0.758
V_{peak} (mV)	-26.0 ± 2.2	-24.0 ± 4.3	0.591
Activation V½ (mV)	-39.3 ± 1.4	-44.2 ± 1.8	0.102
Activation k (mV)	5.3 ± 1.3	3.8 ± 0.7	0.361
Inactivation V½ (mV)	-78.2 ± 2.5	-88.3 ± 2.7	<0.001
Inactivation k (mV)	-6.9 ± 0.4	-9.8 ± 0.7	<0.001
Peak current density at -10 mV (pA/pF)	-154.4 ± 24.0	-33.1 ± 4.7	<0.001
Persistent current density at -10 mV (pA/pF)	-0.61 ± 0.15	-0.55 ± 0.2	<0.01
T_p at -10 mV (ms)	1.4 ± 0.1	1.5 ± 0.2	<0.001
τ_f at -10 mV (ms)	0.9 ± 0.1	1.2 ± 0.1	<0.001
τ_s at -10 mV (ms)	6.6 ± 0.8	20.8 ± 8.5	0.128
τ_r (ms)	4.5 ± 0.4	7.1 ± 0.6	<0.001

588 [1]ESL: eslicarbazepine acetate (300 μM); V_{thres}: threshold voltage for activation; V_{peak}: voltage at
589 which current was maximal; V½: half (in)activation voltage; k: slope factor for (in)activation; T_p:
590 time to peak current; τ_f: fast time constant of inactivation; τ_s: slow time constant of inactivation; τ_r:
591 time constant of recovery from inactivation. The holding potential was -120 mV. Results are mean ±
592 SEM (n = 7-14). Statistical comparisons were made with paired t-tests.

593 **Table 2.** Effect of S-licarbazepine on Na^+ current characteristics in MDA-MB-231 and HEK-$Na_v1.5$
594 cells.[1]

A. MDA-MB-231 cells			
Parameter	*Control*	*S-Lic*	*P value*
V_{thres} (mV)	-34.4 ± 2.0	-35.7 ± 2.0	0.603
V_{peak} (mV)	11.43 ± 4.4	10.0 ± 4.9	0.818
Activation V½ (mV)	-12.9 ± 1.3	-13.7 ± 1.4	0.737
Activation k (mV)	11.0 ± 0.5	11.9 ± 0.8	0.520
Inactivation V½ (mV)	-71.8 ± 2.5	-76.8 ± 2.2	<0.05
Inactivation k (mV)	-6.8 ± 0.9	-6.0 ± 1.2	0.302
Peak current density at -10 mV (pA/pF)	-12.0 ± 3.1	-6.9 ± 2.5	<0.01
Persistent current density at -10 mV (pA/pF)	-1.3 ± 0.4	-0.6 ± 0.2	<0.05
T_p at -10 mV (ms)	4.5 ± 0.4	5.1 ± 0.7	0.103
τ_f at -10 mV (ms)	2.6 ± 0.4	3.8 ± 0.9	0.206
τ_s at -10 mV (ms)	18.5 ± 6.2	29.2 ± 8.2	0.153
τ_r (ms)	6.8 ± 0.4	13.5 ± 1.0	<0.01
B. HEK-$Na_v1.5$ cells			
Parameter	*Control*	*S-Lic*	*P value*
V_{thres} (mV)	-50.0 ± 1.9	-51.3 ± 3.5	0.598
V_{peak} (mV)	-18.0 ± 4.2	-30.0 ± 5.6	<0.001
Activation V½ (mV)	-32.8 ± 3.1	-40.5 ± 3.4	<0.01
Activation k (mV)	5.9 ± 0.9	4.5 ± 1.1	<0.05
Inactivation V½ (mV)	-75.9 ± 2.6	-79.3 ± 4.1	0.116
Inactivation k (mV)	-6.5 ± 0.4	-8.1 ± 0.5	<0.05
Peak current density at -10 mV (pA/pF)	-140.9 ± 26.8	-77.2 ± 17.0	<0.001
Persistent current density at -10 mV (pA/pF)	-0.9 ± 0.2	-0.5 ± 0.2	<0.05
T_p at -10 mV (ms)	1.8 ± 0.5	2.3 ± 0.6	<0.01
τ_f at -10 mV (ms)	1.0 ± 0.0	1.3 ± 0.1	<0.001
τ_s at -10 mV (ms)	6.3 ± 0.5	7.3 ± 0.5	<0.05
τ_r (ms)	5.7 ± 0.7	8.0 ± 1.2	<0.001

595 [1]S-Lic: S-licarbazepine (300 μM); V_{thres}: threshold voltage for activation; V_{peak}: voltage at which
596 current was maximal; V½: half (in)activation voltage; k: slope factor for (in)activation; T_p: time to
597 peak current; τ_f: fast time constant of inactivation; τ_s: slow time constant of inactivation; τ_r: time
598 constant of recovery from inactivation. The holding potential was -120 mV. Results are mean ± SEM
599 (n = 7-14). Statistical comparisons were made with paired t-tests.

600

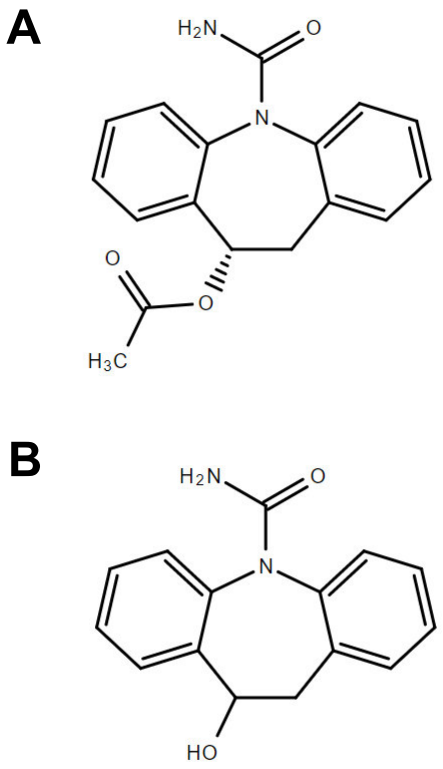

601 Figure 1

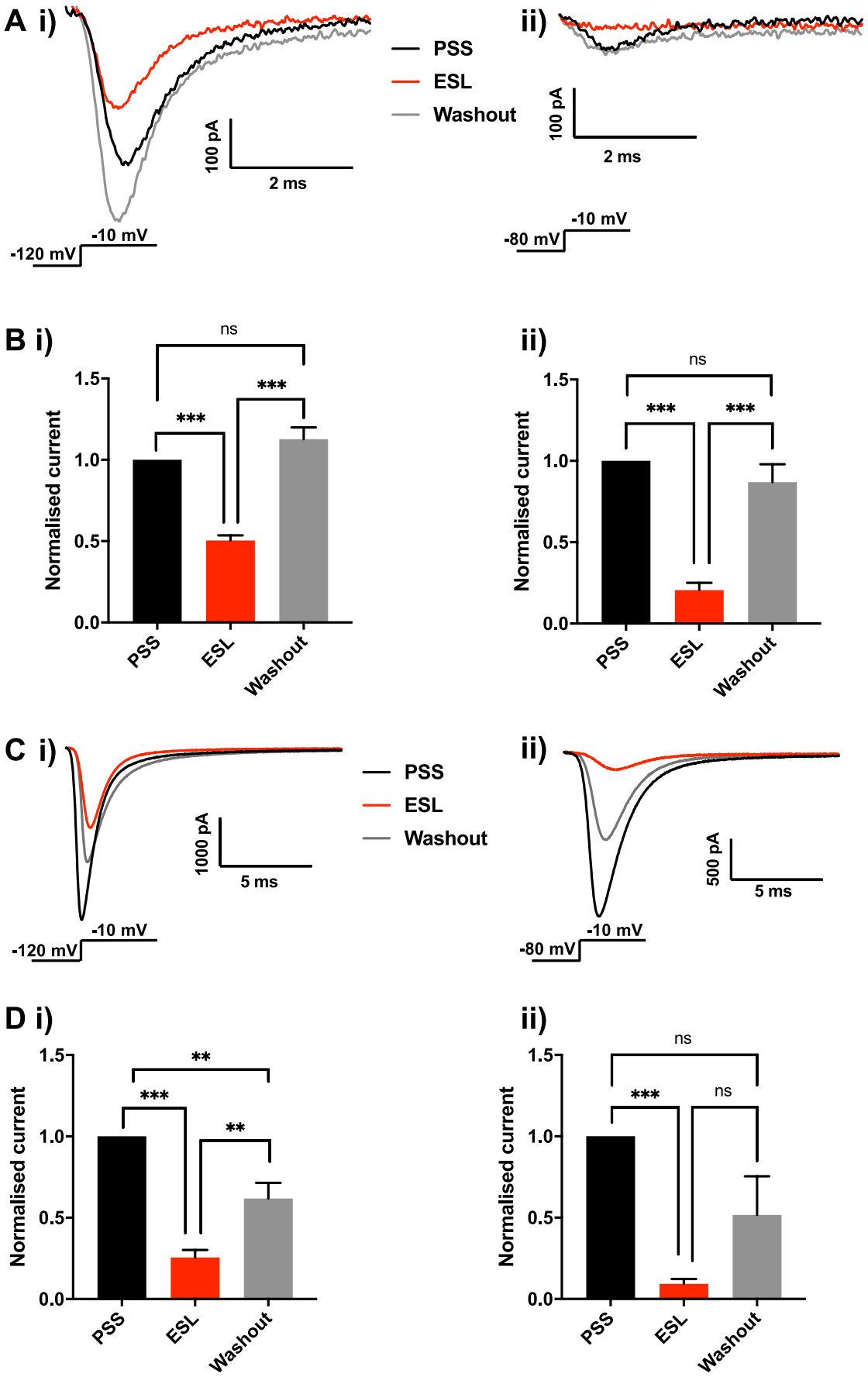
A i)
PSS
ESL
Washout
100 pA
2 ms
-10 mV
-120 mV
ii)
100 pA
2 ms
-10 mV
-80 mV
B i)
ns
***
***
Normalised current
1.5
1.0
0.5
0.0
PSS
ESL
Washout
ii)
ns
***
***
Normalised current
1.5
1.0
0.5
0.0
PSS
ESL
Washout
C i)
PSS
ESL
Washout
1000 pA
5 ms
-10 mV
-120 mV
ii)
500 pA
5 ms
-10 mV
-80 mV
D i)
**
***
**
Normalised current
1.5
1.0
0.5
0.0
PSS
ESL
Washout
ii)
ns
***
ns
Normalised current
1.5
1.0
0.5
0.0
PSS
ESL
Washout

Figure 2

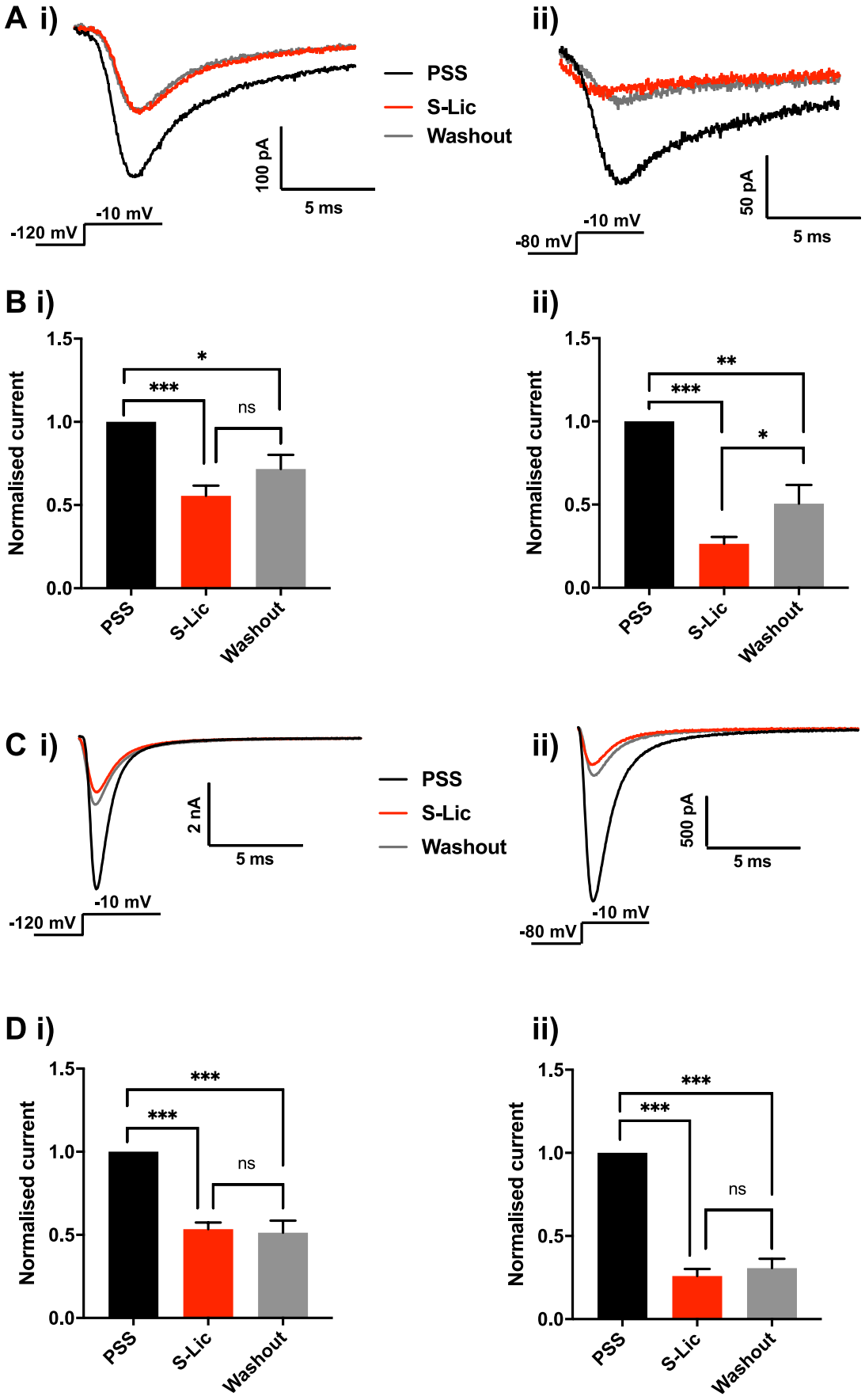
A i)
ii)
PSS
S-Lic
Washout
100 pA
5 ms
-120 mV
-10 mV
50 pA
-80 mV
B i)
ii)
Normalised current
1.5
1.0
0.5
0.0
*
***
ns
**
PSS
S-Lic
Washout
C i)
ii)
2 nA
500 pA
D i)
ii)

603

Figure 3

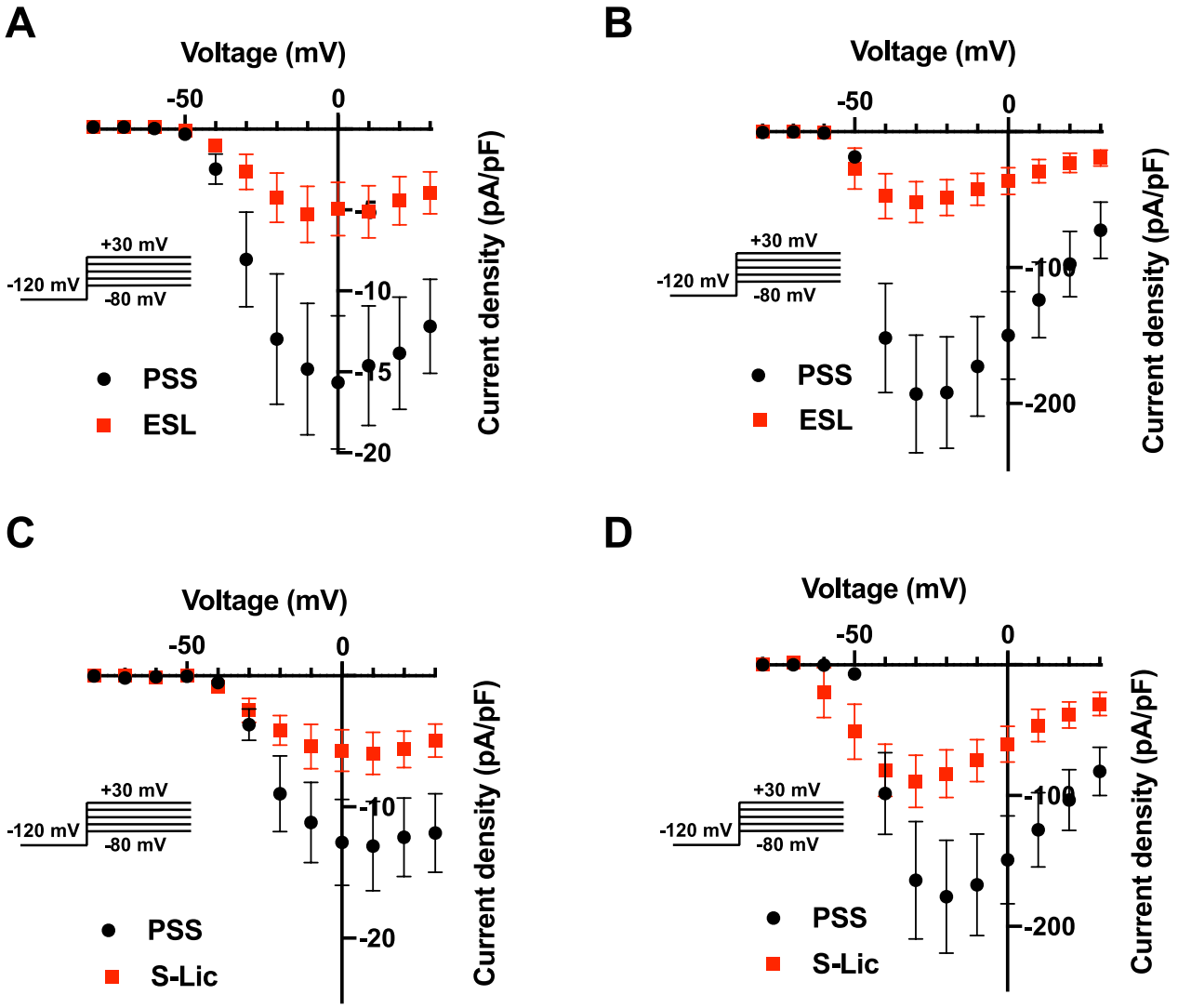
A
Voltage (mV)
-50
0
+30 mV
-120 mV
-80 mV
-10
-15
-20
PSS
ESL
Current density (pA/pF)
B
Voltage (mV)
-50
0
+30 mV
-120 mV
-80 mV
-100
-200
PSS
ESL
Current density (pA/pF)
C
Voltage (mV)
-50
0
+30 mV
-120 mV
-80 mV
-10
-20
PSS
S-Lic
Current density (pA/pF)
D
Voltage (mV)
-50
0
+30 mV
-120 mV
-80 mV
-100
-200
PSS
S-Lic
Current density (pA/pF)

Figure 4

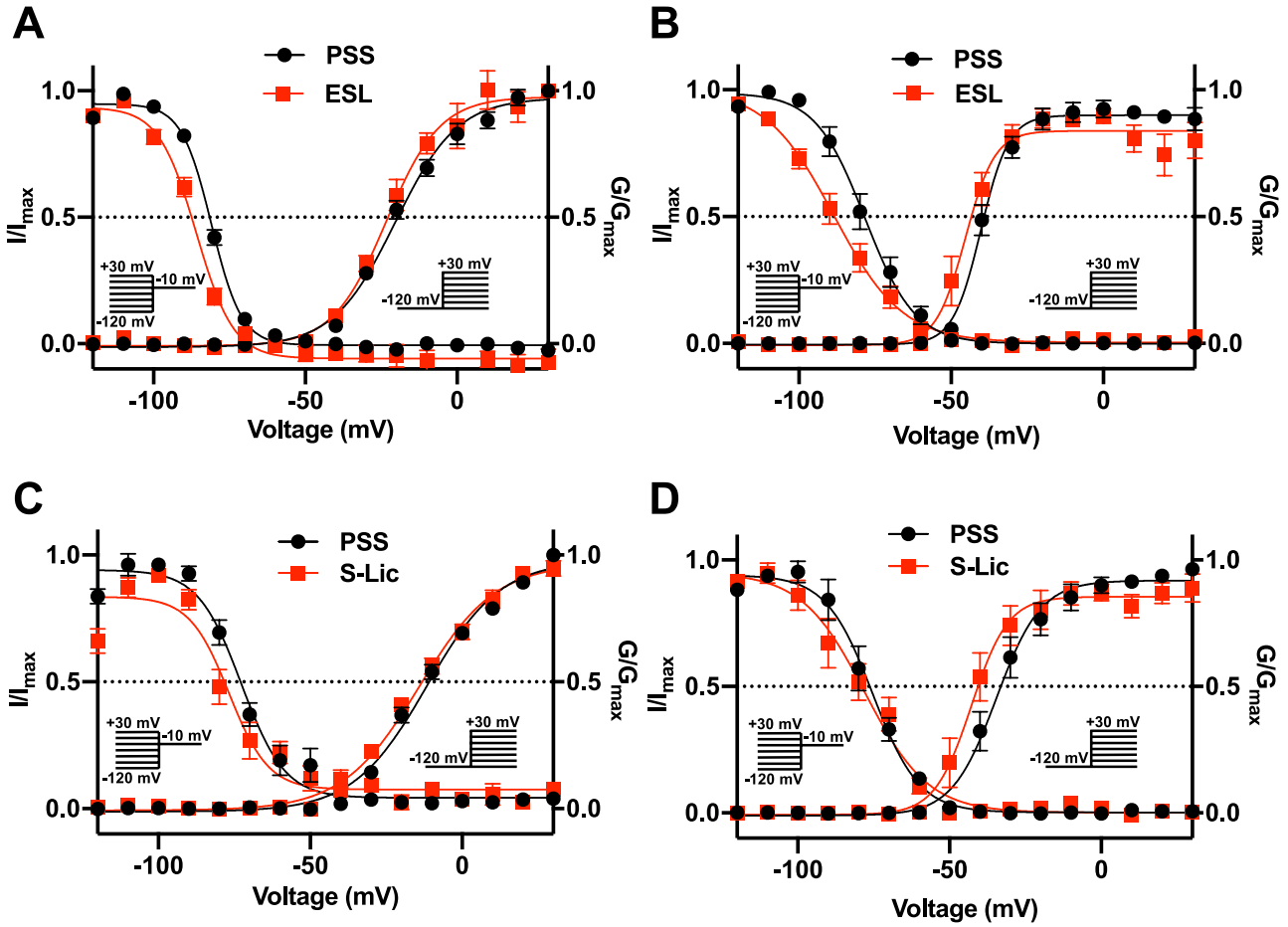
A
PSS
ESL
1.0
0.5
0.0
I/Imax
G/Gmax
+30 mV
-10 mV
-120 mV
+30 mV
-120 mV
-100
-50
0
Voltage (mV)
B
PSS
ESL
C
PSS
S-Lic
D
PSS
S-Lic

Figure 5

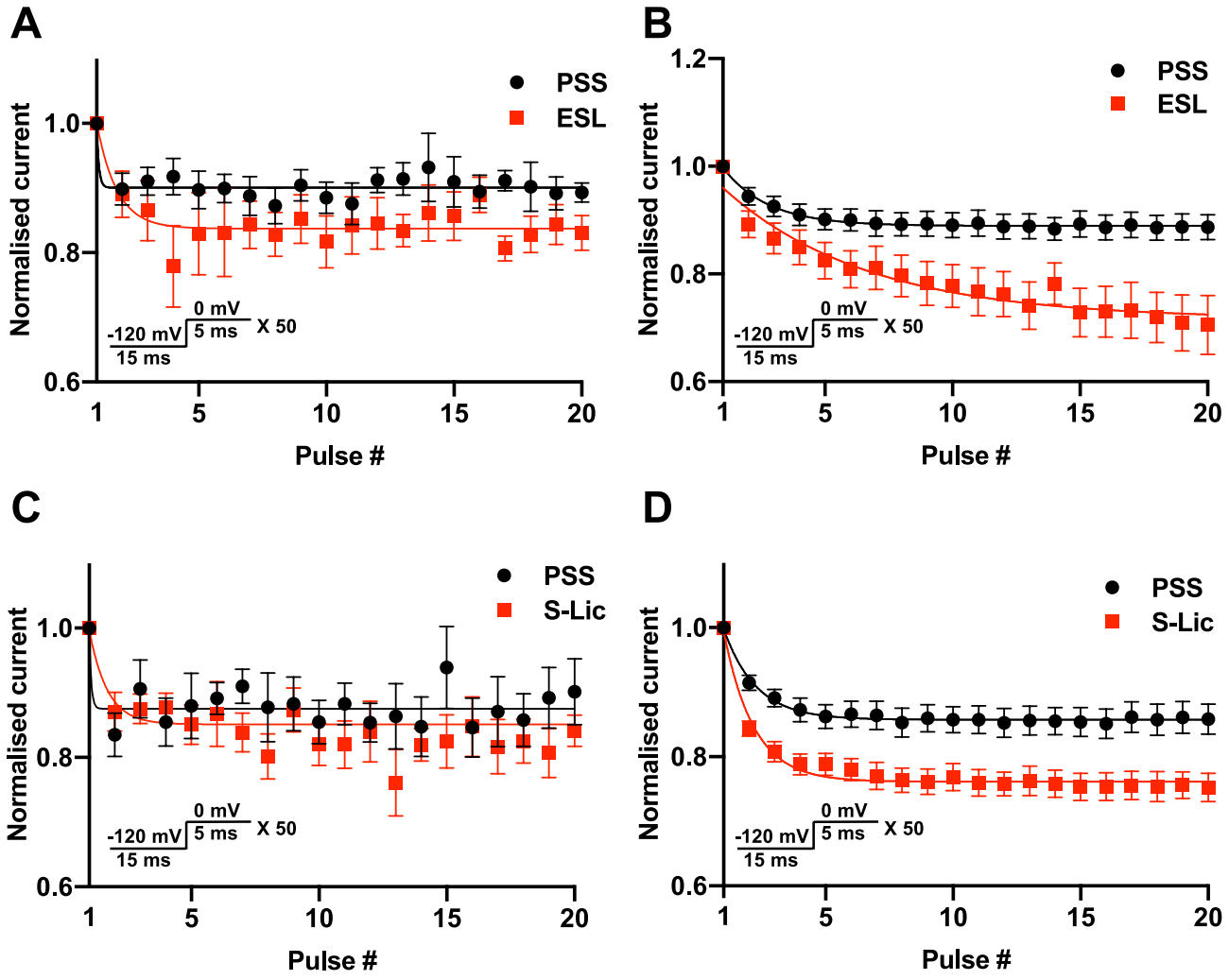
A
B
C
D
PSS
ESL
S-Lic
Normalised current
Pulse #
-120 mV
15 ms
0 mV
5 ms
X 50
1.2
1.0
0.8
0.6
1
5
10
15
20

Figure 6

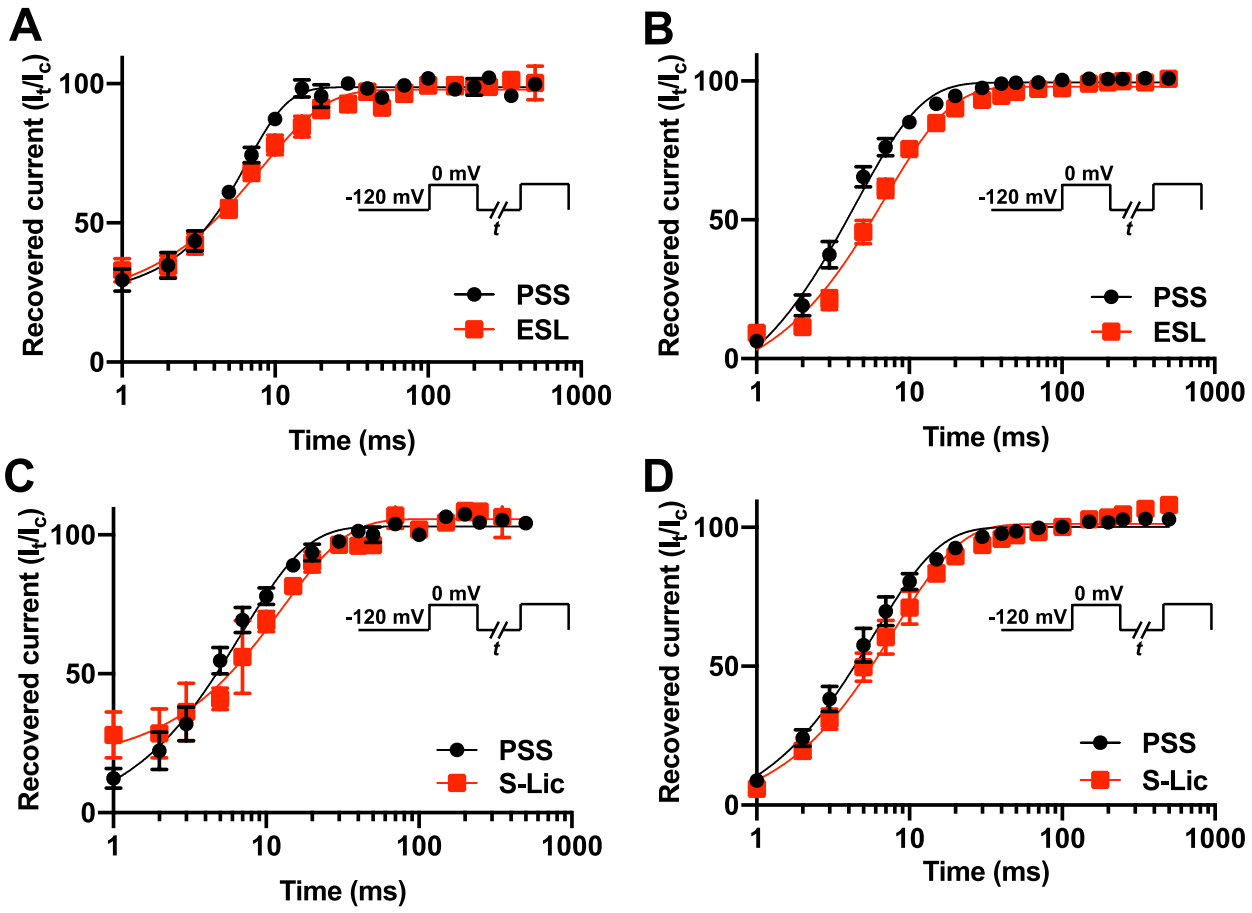

610
611 Figure 7

612

```
SCN2A ATEESAEPLSEDDFEMFYEVWEKFDPDATQFIEFAKLSDFADALDPPLLIAKPNKVQLIA   1841
SCN5A ATEESTEPLSEDDFDMFYEIWEKFDPEATQFIEYSVLSDFADALSEPLRIAKPNQISLIN   1837
      *****:********:****:******:******:: ********. ** *****::.**

SCN2A MDLPMVSGDRIHCLDILFAFTKRVLGESGEMDALRIQMEERFMASNPSKVSYEPITTTLK   1901
SCN5A MDLPMVSGDRIHCMDILFAFTKRVLGESGEMDALKIQMEEKFMAANPSKISYEPITTTLR   1897
      *************:*********************:*****:***:****:*********:
```

Figure 8